Available online at sjuoz.uoz.edu.krd

journals.uoz.edu.krd

Science Journal of University of Zakho

Vol. 11, No. 4, pp. 571 – 580 October-December, 2023

p-ISSN: 2663-628X
e-ISSN: 2663-6298

CLASSIFIED COVID-19 BY DENSENET121-BASED DEEP TRANSFER LEARNING FROM CT-SCAN IMAGES

Walat R. Ibrahima, [a*], Mayyadah R. Mahmood [a]

a,* Faculty of Science, University of Zakho, Zakho, Kurdistan Region, Iraq – (walat.ebrahim@stud.uoz.edu.krd, mayyadah.mahmood@uoz.edu.krd)

Received: 21 June, 2023 / Accepted: 22 Oct., 2023 / Published: 19 Dec, 2023. https://doi.org/10.25271/sjuoz.2023.11.4.1166

ABSTRACT:

The COVID-19 disease, which has recently emerged and has been considered a worldwide pandemic, has had a significant impact on the lives of millions of people and has forced a substantial load on healthcare organizations. Numerous deep-learning models have been utilized for diagnosing coronaviruses from chest computed tomography (CT) images. However, in light of the limited availability of datasets on COVID-19, the pre-trained deep learning networks were used. The main objective of this research is to construct and develop an automated approach for the early detection and diagnosis of COVID-19 in thoracic CT images. This paper proposes the DDTL-COV model, a deep transfer learning model based on DenseNet121, to classify patients on CT scans as either COVID or non-COVID, utilizing weights obtained from the ImageNet dataset. Two datasets were used to train the DDTL-COV model: the SARS-CoV-2 CT-scan dataset and the COVID19-CT dataset. In the SARS-CoV-2 CT dataset, the model achieved a good accuracy of 99.6%. However, on the second dataset (COVID19-CT dataset), its performance shows an accuracy rate of 89%. These results show that the model performed better than alternative methods.

KEYWORDS: DTL, CNN, DenseNet121, COVID-19, Chest CT scan radiography.

1. INTRODUCTION

1.1 Overview

SARS-CoV-2 or COVID-19 is the worldwide epidemic caused by Coronavirus illness in 2019 caused severe acute respiratory syndrome (SARS) and was found for the first time in Wuhan, which is located in China. In March 2020, the World Health Organization (WHO) gave the disease the name COVID-19 and predicted that it would spread over the world as an epidemic (Cantarero et al. 2021;De Anda-Suarez et al. 2022). COVID-19 negatively affects the health of people, especially the elderly, people with existing medical issues, and people whose immune systems are already impaired. By the middle of July 2020, more than 13 million individuals had contracted COVID-19, and more than 570,000 people had already died from the epidemic (Sakib et al. 2020). COVID-19's most pervasive clinical characteristics are a dry cough, fever, and tiredness (Yan et al. 2021). patients often have the most severe symptoms of pneumonia after they have been infected with the coronavirus (Rahman, Khandakar, and Member 2021). Despite this, it is possible that some COVID-19 cases may exhibit no symptoms at all. In severe circumstances, intensive care unit treatment or oxygen support therapy may be required (Munusamy et al. 2021). "Reverse Transcriptase Polymerase Chain Reaction (RT-PCR)" real-time testing was utilized as a diagnostic method to halt the COVID-19 illness from spreading after the genome of SARS-CoV-2 was sequenced (Mondal et al. 2022).

The present pandemic state does not support the low-sensitivity RT-PCR test because RT-PCR takes considerable time and has a significant number of false-negative results (Ibrahim and Mahmood 2023). A test result that is falsely negative can result in an illness spreading extensively (Tabik et al. 2020). Sometimes, infected individuals may not be identified right away and may not receive the proper care (Shah et al. 2021). Consequently, diagnostic imaging, especially chest X-rays and chest computerized tomographic (CT) (Dai et al. 2020), is frequently used in combination with other tests to aid in earlier COVID-19 screening and treatment (Tai et al. 2021).

In light of this, lesions with ground-glass opacities (GGO) and pulmonary fibrosis are COVID-19 lung imaging features (Dong et al. 2021). CT scans are extremely sensitive, so they help assess the severity of the illness; however, their main limitation is the time required for diagnosis; even radiology specialists require approximately 21.5 minutes to parse each case's test results (Wu et al. 2021). For these reasons, automated diagnosis technologies, such as models of deep learning (DL), have been created to screen for COVID-19 in CT images recently (He et al. 2020). According to several recent studies, CNNs are a particular kind of DL technique (Hussain et al. 2021), having a high capability for COVID-19 identification (Shi et al. 2021). With an acceptable performance prediction using COVID-19-infected patients' chest CT scan images (Mohammed et al. 2020). These techniques can be applied by fine-tuning the weights or knowledge gained from the pre-trained CNN model on the large dataset and adapting it to perform well on specific tasks with limited data and achieve better results compared to training from scratch (Shukla et al. 2020). As in the dataset of COVID-19 for the diagnosis of COVID-19 from CT-scan chest images (Sarker et al. 2020). A densely connected convolutional network (DenseNet), a specialized CNN technique, has the advantages of mitigating the problem of vanishing gradients, improving feature reuse, and decreasing parameter usage. Despite these advantages, it has some limitations, such as computational complexity and the substantial amount of GPU memory; furthermore, DenseNet-121 is prone to overfitting (Albelwi 2022).

Therefore, the main focus of this study is on using pre-trained DenseNet-121 models of DL to automatically identify and diagnose COVID-19 using chest CT-scan data.

The following is a list of the important contributions that this article has made:

* Corresponding author

1. The DenseNet121-based Deep Transfer Learning (DTL) model was modified by the exclusion of the last layer (i.e., the top) and the addition of three dense layers, including Dense128, Dense64, and Dense2, to the model to enhance the model and achieve high accuracy.
2. The model is used as an approach for automatically detecting and diagnosing COVID-19 patients on lung CT-scan images.
3. To ensure a precise and effective evaluation of the model, the image datasets go through a pre-processing stage.
4. Employing a modified model on two CT-scan image datasets offers a faster alternative to the widely used RT-PCR testing kit.

The remaining parts of this article have been organized into the following sections and order: The relevant works are listed in section 2. The suggested DTL model and data description are described in Section 3. In section 4 the findings and their analysis are discussed. Finally, section 5 presents the points of conclusion.

2. RELATED WORK

Various study projects have been carried out extensively and fast in order to build AI strategies for combating the COVID-19 worldwide pandemic. Some relevant research on using a chest CT scan to diagnose and classify COVID-19 is reviewed.

Wang, Liu, and Dou (2020) suggested a new joint learning framework to use different datasets to detect COVID-19 disease. The network has been split into two parts. The first part has a lightweight structure and four separate layers of convolution. The second part has more densely packed learning blocks that connect. The COVID-CT dataset and SARS-CoV-2 were used in this work. The work results show that the SARS-CoV-2 dataset outperformed the COVID-CT dataset with an accuracy of 90%, 95% precision, 85% recall, and a 90% F1-score.

Panwar et al. (2020) proposed the VGG model as a type of DTL algorithm to classify COVID-19 positive or negative cases, that utilized three distinct datasets: SARS-COV-2 CT-scan, COVID-chest X-ray, and Chest X-ray radiography. The grad-CAM-based colour representation technique was used by the researchers to make the suggested model more comprehensible and interpretable. Achieved an accuracy of 95%, a sensitivity of 94.4%, and a specificity of 95.84.

Silva et al. (2020) presented a model called Efficient CovidNet applied to lung CT-scan radiography to identify COVID-19 patients, which uses voting techniques and cross-dataset analytics. Experimental results obtained from SARS-COV-2 CT-Scan datasets show a sensitivity of 98.80%, a precision of 99.2%, and an accuracy of 98.99%.

Seum et al. (2020) compared 12 pre-trained CNNs models in classifying COVID-19 patients by utilizing an available dataset (the SARS-COV-2 CT-Scan). This work was carried out in two phases: one without segmentation and another with segmentation. The study results showed in the first phase that the performance of the DenseNet169 model is higher than other models in terms of F1-scores, and accuracy with 88.60% and 89.31%, respectively. In the second phase, DenseNet201 and ResNet18 both obtained an accuracy of 89.92%, implying that using classification after segmentation improves the efficiency of a classification model.

Ramzy, Sherin, and Karma (2021) suggested (COV-CAF), which is a computer-aided framework to identify COVID-19 cases through 3D CT-scan pictures. The researchers combined both DL and traditional techniques in COV-CAF, which has two stages: one for preparatory work and the second one for extracting and classifying. The first stage is focused on 3D CT volumes and proposes an effective cut selection method for selecting useful CT slices, and the second stage uses a recently developed CNN called Norm-VGG16 to extract features automatically. They employed two datasets, the SARS-CoV-2 CT-scan and MosMedData. The findings obtained on the SARS-COV-2 CT scan were 97.59% accuracy and 98.41% sensitivity; whereas, it gained an overall accuracy of 97.76% and an average sensitivity of 96.73% on the MosMedData dataset.

Biswas et al. (2021) conducted a study to use effective transfer learning (TL) algorithms to construct an accurate COVID-19 prediction model on SARS-CoV-2 CT datasets. Initially, they utilized three kinds of (DL) models separately: ResNet50, Xception, and VGG-16, and then combined these three models to increase the model's prediction accuracy. The suggested model has a high F1-score of 99% and an accuracy of 98.79%.

Jaiswal et al. (2021) developed a DTL model to detect COVID-19 infection. It is a DenseNet201 – based model, which was trained before with a massive dataset known as the ImageNet dataset. The provided method produced results with an accuracy of 0.9625, 96.2% recall, 96.2% precision, and a specificity of 96.21%.

Hasan et al. (2021), using CNN, suggested a method to find COVID-19 persons via images from lung scanning. They use the newest updated CNN model (DenseNet-121). The findings showed a satisfactory level of performance for the COVID-19 prediction, with an accuracy of 92% and a recall of 95%.

Horry et al. (2020) built a mechanism for COVID-19 detection based on the DL by utilizing the VGG19 algorithm on various kinds of medical photographs (CT, x-ray, ultrasound), achieving a precision of 84% for CT scans, 86% for x-rays, and 100% for ultrasounds, and this system was able to identify COVID-19 in 100% of the ultrasound images.

Islam and Matin (2020) employed LeNet-5 CNN networks after a simple CNN model to predict COVID-19 from thoracic images. For training purposes, the obtained results were an accuracy of 86.06%, an F1-score of 87%, 89% recall, 85% precision, and a 0.86 ROC.

Pham (2020) showed results from 16 pre-trained CNN models of COVID-19 classification. According to this study, TL led to higher classification rates than data augmentation. ResNet-18 had the best sensitivity (98%), MobileNet-v2 earned the maximum accuracy (95%), and F1-score (96%), and DenseNet-201 had the highest degree of specificity (96%). This research utilized various networks, including ShuffleNet, ResNet-18, DenseNet-201, and MobileNet-v2.

Garain et al. (2021), for COVID-19 screening, created a three-layer DCSNN using CT images. The proposed method obtained a 99% F1 score for the potential-based model. For chest CT images, the suggested SNN-based model outperforms CNN models, but it takes longer to train. Furthermore, in comparison to older DL models, the current method is more efficient.

Chen et al. (2021) conducted a study on automatically identifying positive COVID-19 patients using chest CT scan radiography, a prototype network that has been pre-trained by a momentum-contrasting learning strategy was applied. They obtained values of 87% of accuracy, 93.2% of AUC, 88.5% of precision, and recall 87.4%.

Huang and Liao (2022) proposed LightEfficientNetV2 model and fine-tunes seven CNN techniques involving EfficientNet-B0, InceptionV3, Xception, MobileNetV2, DenseNet121, EfficientNetV2, and ResNet50V2 to diagnose COVID-19 cases on three different datasets (NIH Chest X-rays, SARS-CoV-2, and COVID-CT). The proposed LightEfficientNetV2 model obtained an accuracy of 99.47% on the SARS-CoV-2 dataset and 88.67% on COVID-CT.

Kathamuthu et al. (2023) used several deep transfer learning-based CNN approaches including InceptionV3, Resnet50, Xception, VGG16, VGG19, and Densenet121 to screen COVID-

19 in chest CT images and achieved an accuracy of 98% with VGG16 model on SARS-CoV-2 CT-scan dataset.

3. METHODOLOGY

In light of the limited number of COVID-19 radiography pictures in our dataset, it is difficult to develop a DL model in this situation because DL approaches need a huge dataset to start from scratch. Transfer learning (TL) could be utilized as an effective solution to this issue because TL techniques use the knowledge gained in one field to carry out tasks in other fields. For instance, when initializing DL models with weights obtained from the ImageNet (Fei-Fei, Deng, and Li 2010), as the ImageNet is a massive dataset comprised of 14 million images from various resources, by that time it has learned several features for diverse images, so these newly acquired features can then be applied to another dataset. For this reason, the weights gained from pre-trained DenseNet-121 on the ImageNet dataset were employed for the SARS-COV2 and the COVID19-CT datasets in this study.

3.1 Study Design

The study system's processes start with two distinct datasets that go through data pre-processing techniques before being split into training, validation, and test sets. Hence, the data are ready to fit into a modified model. Figure 1 shows the general study diagram.

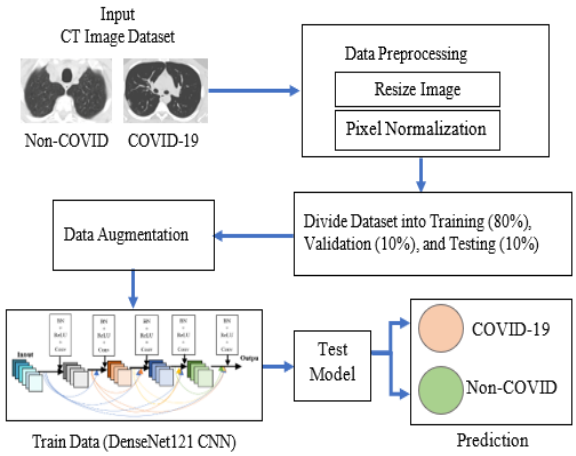

Figure 1: The general study diagram.

3.2 Datasets Description

The two datasets that were utilized in this paper are demonstrated in this section. It provides details about the source, size, nature, characteristics, and other information of the datasets.

3.2.1 SARS-CoV-2 CT-scan dataset: This dataset consists of a total of 2481 CT scans from 120 patients, including 1252 CT scan images of 60 infected persons (COVID-19), 28 females with

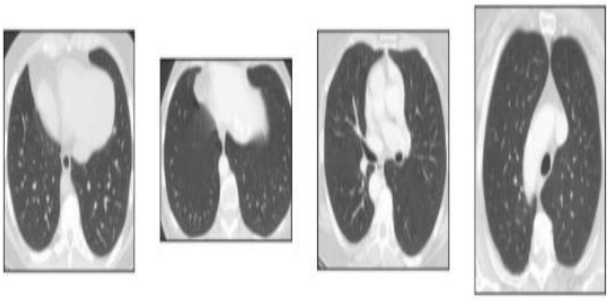

32 males, and 1229 CT scan images of 60 uninfected persons (non-COVID), females (30) and males (30) (Soares and Angelov 2020). Figure 2 shows samples from each class (non-COVID and COVID-19). These data were obtained from patients in Sao Paulo hospitals, Brazil. There are no standard dimensions for CT-scan images; in general, their sizes are between 104 × 153 and 484 × 416. Figure 3 shows the different sizes between them. The protocol offered for evaluating models is split randomly into training, validation, and testing at 80, 10, and 10 percent, respectively, by the train_test_split () method. The distribution of the dataset is shown in Table 1. The dataset can be found at: www.kaggle.com/plameneduardo/sarscov2-ctscan-dataset.

Figure 2: Non-COVID (left) and COVID-19 (right).

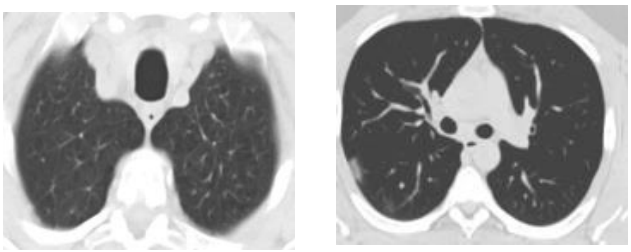

Figure 3: CT-scan images of different sizes.

3.2.2 COVID19-CT dataset: The second dataset comprises 216 instances of COVID-19 and 171 cases of non-COVID, with a collection of 746 CT scans. Among the CT scans, there are 349 images of instances of COVID-19 with 397 samples of non-COVID-19, including several other disorders of the lungs (He et al. 2020). Positive CT scans had been sourced from preprints on COVID-19 available on bioRxiv and medRxiv, displaying a range of symptoms. As the CT scans were obtained from various places, their dimensions varied from 124 × 153 to 1485 × 1853, causing inconsistencies in image contrast, as shown in Figure 4. The pattern of the spreading of the dataset is displayed in Table 1. The data are available at : https://www.kaggle.com/datasets/luisblanche/covidct?resource=download&select=CT_NonCOVID.

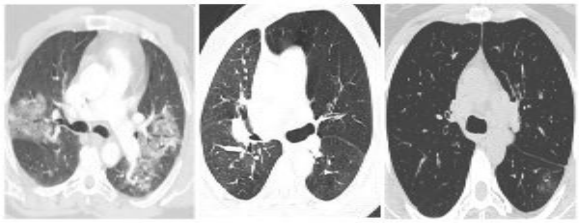

Figure 4: The differences in contrast CT scan images.

Table 1: The pattern of distribution of the SARS-COV-2 CT-scan and COVID19-CT datasets.

Dataset	SARS-COV-2 Ct-Scan	COVID19-CT
# Patients	120	387
# CT-scan images	2481	746
Train sets images	1983	596
Valid sets images	249	75
Test sets images	249	75

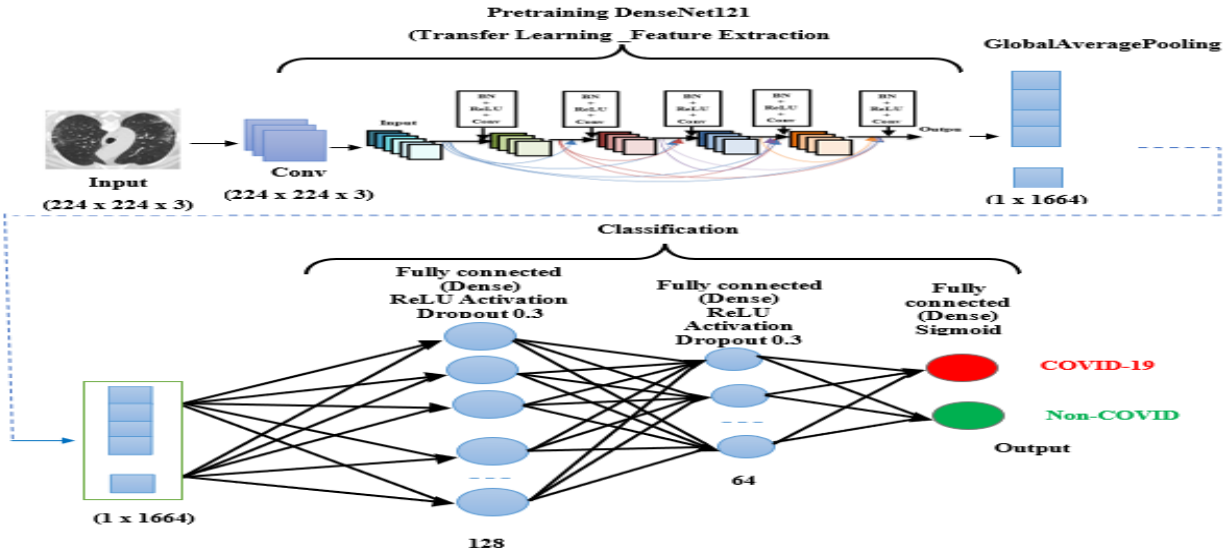

Figure 5: The DDTL-COV model's structure, which includes DenseNet121

3.3 Data Pre-processing

The term used to describe all the changes made to initial data before feeding it into machine learning (ML) or DL algorithms named pre-processing. All images are resized from different resolutions to 224 x 224 resolution using the OpenCV library interpolation function INTER_AREA. Additionally, the pixels' values might range from 0 to 255. If a DL model is applied to the image as-is, computing high numeric values may become more challenging. We can minimize this by adjusting the values to be between 0 and 1, also known as normalization, which is a significant stage to guarantee that each input parameter (in this case, a pixel) has a uniform data distribution. This makes convergence faster while training the network.

3.4 Data Augmentation Techniques

In data analysis, data augmentation is utilized to raise the number of training data sets either by producing drastically altered copies of already existing data or by developing synthetic data from earlier existing data. This is accomplished by one of these two methods. This technique enhances the generalization performance and classification accuracy of the model while also serving as a regularise to reduce overfitting (Tang, Yuan, and Zhu 2020). Table 2 lists the parameters used for image augmentation in the current study.

3.5 The Modified DenseNet121

In this study, a DenseNet121-based Deep Transfer Learning model-COVID-19 is modified and called (DDTL-COV) to classify COVID-19-infected patients from chest CT-scan images. The DDTL-COV was trained using TL, with the pre-trained.

DenseNet121 weights on the ImageNet dataset used as the initial weights. Following this, the model was fine-tuned on the COVID-19 dataset. Figure 5 shows the architecture of the DDTL-COV model, which employs DenseNet121 for accurately classifying COVID-19 patients.

The main parts of the DDTL-COV model are the feature extraction and classification parts.

In the feature extraction part, the input layer of the CNN is defined by the shape of the input image (224,224,3) followed by a convolutional layer of 3 kernels with size (3 x 3) with padding 'same'. The DDTL-COV model was trained using TL with the pre-trained DenseNet121 weights on the ImageNet dataset.

Table 2: Parameters for image augmentation

Parameters	values	Functions
Rotation-range	360	The degree range of rotations randomly
Width-shift-range	0.2	The range of shifting horizontally is randomly selected.
Height-shift-range	0.2	The range of shifting vertically is randomly selected.
Horizontal-flip	True	The input randomly flips in the horizontal direction.
Vertical-flip	True	The input randomly flips in the vertical direction.
Zoom range	0.2	The randomized zooming range.

DenseNet is a logical extension of ResNet and boosts performance by merging the feature maps at each layer with those of the layer that came before it inside a dense block. This permits the layers of the network that come after them to directly use the features of the layers that came before them, which promotes the reuse of features across the network as shown in Figure 6, which facilitates solving the vanishing gradient issue and also minimizes the parameters' number.

Depending on the network version, the DenseNet network is structured into four blocks of layers, each of which has a particular number of layers. For instance, the DenseNe-169 has 4 blocks with 6, 12, 32, and 32 layers, respectively, and DenseNe-121 was used in this study; it is shown in **Error! Reference source not found.** 7 as having four blocks with a total of 6, 12, 24, and 16 layers, respectively.

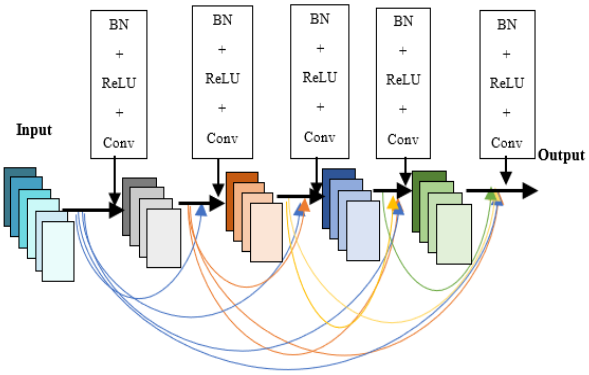

Figure 5: A dense block with five layers that shows the direct connections between layers.

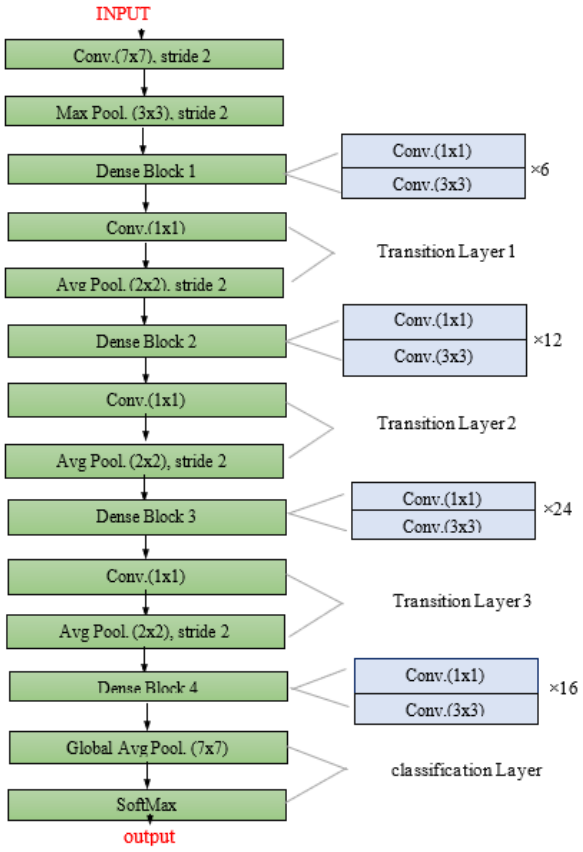

Figure 6: DenseNet121's layered architectural design.

Layers for Batch Normalization, Relu functions, consonant layers, and Pooling layers are put between these blocks.

The DenseNet121 architecture implements direct interconnections between all antecedent and subsequent layers in furtherance of connectivity.

The feature concatenation's mathematical formulation is as follows:

$$u^l = H_l([u^0, u^1, \dots\dots, u^{l-1}]) \quad (1)$$

Here, $H_l(.)$ is a transition that is not linear. It consists of BN and ReLU (Yu et al. 2020). And mathematically can be represented as in Eq (2)

$$\mathrm{ReLU}(x) = \begin{cases} 0, & x < 0 \\ x, & x \geq 0 \end{cases} \quad (2)$$

And followed by a convolution layer of (3 x 3) windows, $[u^0, u^1, \ldots\ldots, u^{l-1}]$) is the feature map string for layers 0 to l-1 that has been concatenated into one tensor for simplicity of use, for down sampling. In the model architecture, transition layers made up of a BN layer are used to build and separate dense blocks, a 2×2 average pooling layer at the end, and a (1×1) convolution layer between them.

The growth rate, represented by the hyperparameter k in DenseNet121, indicates how the dense design achieves superior outcomes. The architecture of DenseNet121 evolves by observing feature maps as the network's global state. Therefore, despite having a reduced growth rate, it performs efficiently. Every succeeding layer of the network is able to access all of the feature maps that were generated by the layer that came before it. Additionally, each layer adds k feature maps to the overall state, resulting in a total input feature map count across the l^{th} layer known as FM:

$$(FM)^l = K^0 + K(l-1) \qquad (3)$$

Here, k^0 is the symbol for the channels on the input layer. To improve the efficiency of computation, an (1x1) convolution layer is added before every (3x3) convolution, decreasing the number of inputs for the feature map, which is typically more than the number of output feature maps k. The bottleneck layer, which is a (1x1) convolution layer, is inserted and creates 4k feature maps.

In the classification part, the fully connected layer at the end pre-trained DenseNet121model (i.e., the top) is excluded (include_top = False), an additional three dense layers including (Dense128_Relu_BN_Dropout 0.3), (Dense64_Relu_BN_Dropout 0.25), and last dense (2) is added to the model after GobalAveragePooling2D layer and BN, hence, Dense () indicates the layer's neurons, BN represents the Batch Normalization layer, Relu is the activation function, Dropout () is used to regularize CNNs in addition, it overcomes the over-fitting issue. For binary classification, the last Dense layer along the sigmoid is utilized as the output layer since the sigmoid is an activation function that turns non-normalized outputs into binary 0s and 1s, where (0 = COVID-19, 1= Non_COVID).
The sigmoid function can be expressed using the formula below:

$$y = \frac{1}{1 + e^{-(\sum w_i x_i)}} \qquad (4)$$

The history of the model is presented in Table 3.

Table 3: Model history.

Layer(type)	Output shape	Parameter #
Input layer	(None,224,224,3)	0
Conv2D	(None,224,224,3)	84
Densenet121 (Functional)	(None, None, None, 1024)	7037504
GlobalAveragePooling2d	(None, 1024)	0
Batch normalization	(None, 1024)	4096
Dense	(None, 128)	131200
Batch normalization_1	(None, 128)	512
Dropout	(None, 128)	0
Dense 1	(None, 64)	8256
Batch normalization_2	(None, 64)	256
Dropout 1	(None, 64)	0
Dense 2	(None, 2)	130
Total parameters: 7,182,038 Trainable parameters: 7,095,958 Non-trainable parameters: 86,080		

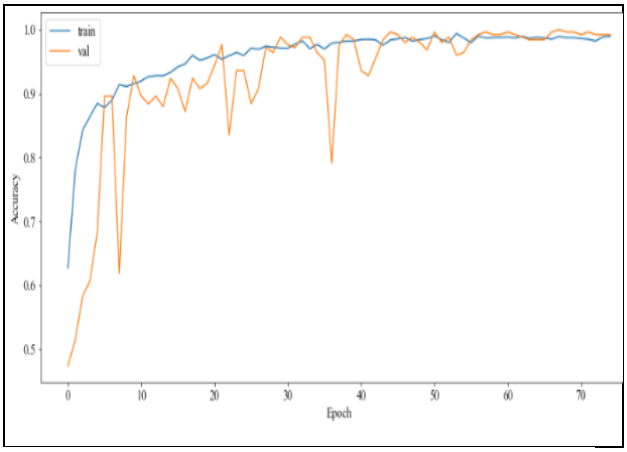

Figure 7: The accuracy of the DDTL-COV model throughout training and validation across the course of 75 epochs.

3.6 Hyperparameters

The model completed training around 20 minutes with 75 epochs and a batch size of 32. The binary cross-entropy is utilized as a loss function that is capable of being lowered using the backpropagation approach while the model is being trained. The following equation demonstrates the loss function:

$$L(\theta) = -\frac{1}{n}\left[\sum_{i=1}^{n}\sum_{k=1}^{k} y_k^i \ln h_\theta\left(x^i\right)_k\right] \qquad (5)$$

Here, the number of training samples is represented by n, the number of classes by k, the model parameter is θ, the actual level of the i^{th} training sample is y_k^i, and the output for the i^{th} training sample is $h_\theta\left(x^i\right)_k$ at the k^{th} node.

The model is optimized by using the Adam optimizer, which is a subset of the stochastic gradient descent approach that is based on adaptive estimation of the first moment estimate m_t, second-moment estimate v_t, with α = 0.003 as the initial learning rate. updating the model weight θ with Adam's optimizer is illustrated in the below equation:

$$\theta_t = \theta_{t-1} - \alpha\frac{m_t}{\sqrt{v_t}+\varepsilon} \qquad (6)$$

Where

$$m_t = \beta_1 \times m_{t-1} + (1-\beta_1) \times g_t \qquad (7)$$

$$v_t = \beta_2 \times v_{t-1} + (1-\beta_2) \times g_t^2 \qquad (8)$$

Here, g_t represents the weights of the gradient concerning the loss function, the weight at time t−1 is indicated by θ_{t-1}, the weight at time t is represented by θ_t, β_1, and β_2 are hyperparameters, the default value of $\beta_1 = 0.9$ and $\beta_2 = 0.999$ were used, With the ReduceLROnPlateau callback, the learning rate is decreased by a factor of 0.70 until it reaches a lower limit (min lr = 0.0001) when the validation loss remains constant for about 5 epochs (patience = 5).

4. RESULTS AND DISCUSSIONS

4.1 Introduction

This section demonstrates the efficacy of the suggested model in identifying if a person has COVID-19 illness or not by using the datasets SARS-CoV-2 CT-scan and COVID19-CT. Initially, we analyzed SARS-CoV-2 CT results then COVID19-CT and compared them. Additionally, each dataset's results were then compared with those from earlier studies and research using the same datasets. The pretraining model that is used in this study is DenseNet-121.

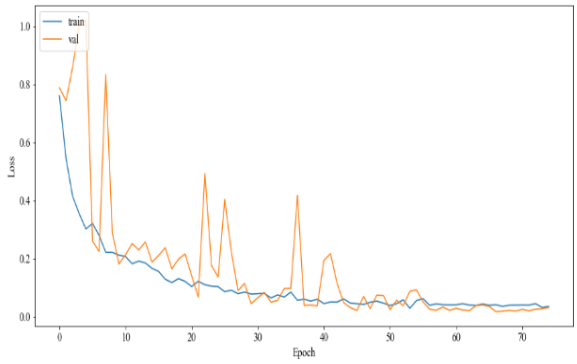

Figure 8: The loss of the DDTL-COV model throughout training and validation across the course of 75 epochs.

4.2 Experimental setup

In this study, a Windows 10 Pro 64-bit operating system has been used with the Anaconda compiler supported by Python 3.7 and the TensorFlow library and Keras library, which both support GPU hardware acceleration on some COVID-19 CT scans for DL and CNN purposes, probably for achieving perfect infection detection. And, as for hardware, the following computer and key specifications were used: I5-10400F (10th Generation Intel Core i5 Desktop Processor with 6 cores and 12 threads), GeForce RTX 2070 with 8GB of vRAM, and 16 GB of DDR4 at 2666 MHz (RAM/Memory).

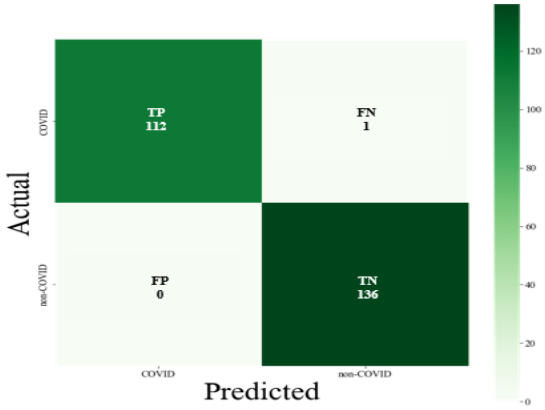

Figure 9: Confusion matrix of the DDTL-COV model for the SARS-CoV-2 CT dataset.

4.3 The results of the DDTL-COV model from the SARS-CoV-2 CT dataset

Three sets are created from the dataset for the performance analysis. 80% of the data used to train the model is in the training set. 10% of the data makes up the validation set, which is used to fine-tune the model's hyperparameters and guard against overfitting. The remaining 10% of the data makes up the testing set, which is used to assess the model's ultimate performance. The loss of training and validation decreases gradually through each epoch, indicating that the model is learning and generalizing well. After epoch 55, the validation loss stops decreasing, which means that the model has reached its optimal performance. It is crucial to remember that the ideal number of epochs may change based on the model's complexity and the quantity of the dataset. The training and validation accuracy of the DDTL-COV model across various epochs are arranged in Figure 8, and the loss analyses of the model over the same number of epochs is illustrated in Figure 9.

Figure 10 shows a confusion matrix that is used to summarize the results of samples of each class that were successfully and mistakenly categorized. Based on the confusion matrix, the performance of the model was evaluated using four metrics: precision, recall, F1 score, and accuracy. The DDTL-COV model only produced one false positive case and no false negative cases, indicating a high score of accuracy of 99.6% and an F1-score of 100%. So, it will be of significance in the medical research field, as shown in Table 4.

Table 4: DDTL-COV model results from the SARS-CoV-2 CT dataset.

Class\metrics	precision	recall	F1-score
Class 0\COVID-19	100%	99%	100%
Class 1\non-COVID	99%	100%	100%
Accuracy overall	100%		
Macro avg	100%	100%	100%
Weighted avg	100%	100%	100%

4.3.1 Comparison of Results with previous studies

In this research, several innovative approaches developed for COVID-19 identification using the SARS-CoV-2 dataset are compared, as shown in Table 5. Some studies yielded fewer results, such as Panwar et al. (2020), which used the VGG model to obtain an accuracy of 95% and a recall of 94.4%. Wang, Liu, and Dou (2020) used the CNN model and achieved 95% accuracy and a 94.4% of F1-scor. As for Ramzy, Sherin, and Karma (2021), with VGG16, accuracy is 97.59%, recall is 98.41%, and so on. On the other hand, some other studies introduced various DL models and got superior results, as Silva et al. (2020) were capable to obtain an accuracy of 98.99%, a recall of 98.80%, and a precision of 99.20% through the utilization of Efficient CovidNet, and Biswas et al. (2021), by merging three previously trained CNNs of models (Xception, ResNet50, and VGG-16), were able to get an F1-score of 99% and an accuracy of 98.79%. The overall performance of the DDTL-COV model is superior to all other studies.

Table 5: A comparison of the DDTL-COV model with the modern techniques using the SARS-CoV-2 CT dataset (Acc: accuracy, Pre: precision, Rec: recall, F1-S: F1-score).

Ref.	Method	Acc. %	Pre. %	Rec. %	F1-S %
(Wang, Liu, and Dou 2020)	CNN	90	95	85	90
(Panwar et al. 2020)	VGG	95	/	94.4	/
(Silva et al. 2020)	Efficient CovidNet	98.99	99.20	98.80	/
(Seum et al. 2020)	12 pre-training CNNs	89.92	99.50	86.80	89.67
(Ramzy, Sherin, and Karma 2021)	VGG16	97.59	/	98.41	/
(Biswas et al. 2021)	Combine 3 pre-trained CNNs models (VGG-16, ResNet50, Xception)	98.79	/	/	99
(Jaiswal et al. 2021)	DenseNet201	96.21	96.25	96.2	96.2

(Hasan et al. 2021)	DenseNet-121	92	/	95	/
(Huang and Liao 2022)	LightEfficientNetV2	99.47	99.19	99.25	99.04
(Kathamuthu et al. 2023)	VGG16	98	97.99	97.99	97.99
This work	DDTL_COV (DenseNet-121)	99.6	100	100	100

4.4 DDTL-COV model results from the COVID19 CT dataset

As in a previous experiment, the COVID19 CT dataset is partitioned randomly into three distinct sets of training, validation, and testing at 80, 10, and 10 percent, respectively. The model is trained over 75 epochs at a speed of 5 seconds per epoch, and its convergence is at a noticeably good speed. Figures 11 and 12 illustrate the accuracy of training and validation, as well as the training loss, and the validation loss of the DDTL-COV model on the COVID19-CT dataset, respectively.

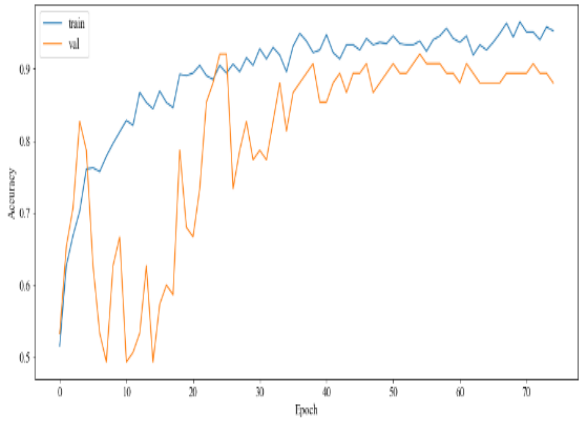

Figure 10: The DDTL-COV model accuracy across 75 epochs of training and validation from the COVID19-CT dataset.

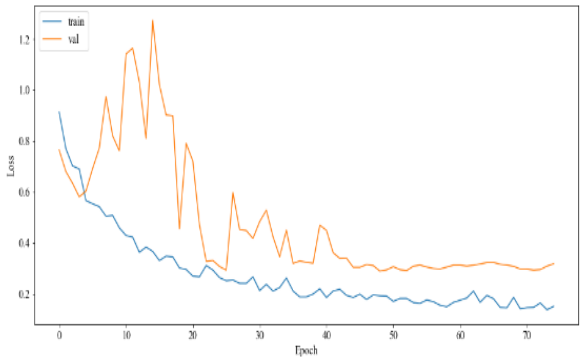

Figure 11: The loss of the DDTL-COV model throughout training and validation across the course of 75 epochs using the COVID19 CT dataset.

Common assessment criteria such as F1-score, Recall (sensitivity), accuracy, and specificity were used to assess the efficacy of the classification method employed in this research. The results of the model are shown in Table 6, which finds that it has a recall of 91% and an accuracy of 89%. Furthermore, these findings show that this model only produced one false negative case and seven false positive cases, as shown in Figure 13.

Table 6: The DDTL-COV model's classification from the COVID19-CT dataset.

Class \ Metrics	Precision	Recall	F1-score
Class 0\COVID-19	81%	97%	88%
Class 1\non-COVID	97%	84%	90%
Accuracy overall 89%			
Macro avg	89%	91%	89%
Weighted avg	91%	89%	89%

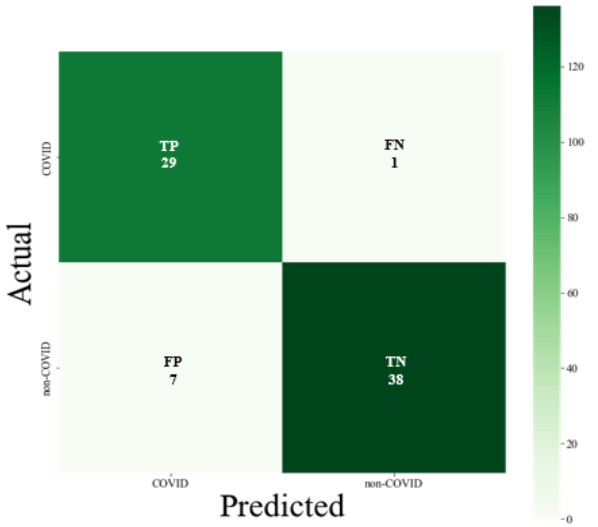

Figure 12: The DDTL-COV model confusion matrix utilizing COVID19-CT dataset.

4.4.1 Result in comparison with previous studies :Compared to the related works using the dataset COVID19 CT, the provided approach obtains average accuracy and F1- scores of 89% and 88%, respectively. The results of some research are fewer (Islam and Matin 2020) which used the basic CNN model plus the LeNet-5 CNN model to achieve an accuracy of 86.06%, a precision of 85%, a recall of 89%, and an F1-score of 87%. Also, its performance is superior to Horry et al. (2020) but less than that to Garain et al. (2021), Chen et al. (2021), and Pham (2020), as shown in Table 7.

4.5 A Comparison of results between the COVID-19-CT dataset and the SARS-CoV-2 dataset

The overall performance of the COVID19-CT dataset in the manner of accuracy in comparison to that of the SARS-CoV-2 dataset is less as shown in Table 8. This is explained by the cross-source variability of the dataset's CT scans. The non-COVID-19 CT images were obtained from various sources and display a variety of results, making it challenging to differentiate between COVID-19 and other findings associated with lung disorders due to the possibility of visual manifestations overlapping. Another explanation is that the COVID19-CT dataset's CT images exhibit a significant contrast variation, varying spatial resolution, and

other visual traits that can impair the model's capacity to extract more discriminative and generalizable features.

Table 7: A comparison of the DDTL-COV model with the modern techniques using the COVID19-CT dataset (Acc: accuracy, Pre: precision, Rec: recall, F1-S: F1-score).).

Ref.	Method	Acc. %	Pre. %	Rec. %	F1-S %
(Horry et al. 2020)	VGG19	/	84	/	78
(Islam and Matin 2020)	CNN + LeNet-5	86.06	85	89	87
(Pham 2020)	Sixteen pre-trained CNNs	95 % (MobileNet-v2)	/	98 (ResNet-18)	96 (MobileNet-v2)
(Garain et al. 2021)	Three-layer DCSNN	/	/	/	99
(Chen et al. 2021)	prototypical network	93.2	88.5	87.4	/
(Huang and Liao 2022)	LightEfficientNetV2	88.67	87.28	87.43	87.55
This work	DDTL_COV (DenseNet-121)	89	89	91	89

Table 8: Accuracy of the DDT-COV model for two datasets on test data.

Datasets	Accuracy
SARS-CoV-2 CT	99.6%
COVID19- CT	89%

CONCLUSION

This study suggests the DDTL-COV model, a deep transfer learning model based on DenseNet121, using weights from the ImageNet dataset to categorize patients on CT scans as either COVID or non-COVID. The SARS-CoV-2 CT scan and COVID19-CT datasets were utilized to assess the model, with image enhancement in pre-processing using the OpenCV library interpolation function INTER_AREA and data augmentation techniques. The suggested model achieves outstanding performance in the SARS-CoV-2 CT-scan dataset, with an accuracy of 99.6%. However, on the COVID19-CT dataset, it performed with an accuracy rate of 89%. The limitation of this model, its performance is not good on the COVID19-CT dataset.

The future study will design a structure combining DL models that have already been pre-trained. Additionally, the technique of k-fold cross-validation will be used as a partitioning strategy for the dataset

REFERENCES

Albelwi, Saleh A. 2022. "Deep Architecture Based on DenseNet-121 Model for Weather Image Recognition." *International Journal of Advanced Computer Science and Applications* 13(10): 559–65.

De Anda-Suarez, Juan et al. 2022. "A Novel Metaheuristic Framework Based on the Generalized Boltzmann Distribution for COVID-19 Spread Characterization." *IEEE Access* 10: 7326–40.

Biswas, Shreya et al. 2021. "Prediction of Covid-19 from Chest Ct Images Using an Ensemble of Deep Learning Models." *Applied Sciences (Switzerland)* 11(15).

Cantarero, Ruben et al. 2021. "COVID19-Routes: A Safe Pedestrian Navigation Service." *IEEE Access* 9: 93433–49.

Chen, Xiaocong et al. 2021. "Momentum Contrastive Learning for Few-Shot COVID-19 Diagnosis from Chest CT Images." *Pattern Recognition* 113: 107826. https://doi.org/10.1016/j.patcog.2021.107826.

Dai, Hui et al. 2020. "High-Resolution Chest CT Features and Clinical Characteristics of Patients Infected with COVID-19 in Jiangsu, China." *International Journal of Infectious Diseases* 95: 106–12. https://doi.org/10.1016/j.ijid.2020.04.003.

Dong, Di et al. 2021. "The Role of Imaging in the Detection and Management of COVID-19: A Review." *IEEE Reviews in Biomedical Engineering* 14: 16–29.

Fei-Fei, L., J. Deng, and K. Li. 2010. "ImageNet: Constructing a Large-Scale Image Database." *Journal of Vision* 9(8): 1037–1037.

Garain, Avishek et al. 2021. "Detection of COVID-19 from CT Scan Images: A Spiking Neural Network-Based Approach." *Neural Computing and Applications* 1. https://doi.org/10.1007/s00521-021-05910-1.

Hasan, Najmul, Yukun Bao, Ashadullah Shawon, and Yanmei Huang. 2021. "DenseNet Convolutional Neural Networks Application for Predicting COVID-19 Using CT Image." *SN Computer Science* 2(5): 1–11. https://doi.org/10.1007/s42979-021-00782-7.

He, Xuehai et al. 2020. "Sample-Efficient Deep Learning for COVID-19 Diagnosis Based on CT Scans." *IEEE Transactions on Medical Imaging* XX(Xx): 10.

Horry, Michael J. et al. 2020. "COVID-19 Detection through Transfer Learning Using Multimodal Imaging Data." *IEEE Access* 8: 149808–24.

Huang, Mei Ling, and Yu Chieh Liao. 2022. "A Lightweight CNN-Based Network on COVID-19 Detection Using X-Ray and CT Images." *Computers in Biology and Medicine* 146(March): 105604. https://doi.org/10.1016/j.compbiomed.2022.105604.

Hussain, Emtiaz et al. 2021. "CoroDet: A Deep Learning Based Classification for COVID-19 Detection Using Chest X-Ray Images." *Chaos, Solitons and Fractals* 142: 110495. https://doi.org/10.1016/j.chaos.2020.110495.

Ibrahim, Walat Ramadhan, and Mayyadah Ramiz Mahmood. 2023. "COVID-19 Detection Based on Convolution Neural Networks from CT-Scan Images : A Review." 29(3): 1668–77.

Islam, Md Rakibul, and Abdul Matin. 2020. "Detection of COVID 19 from CT Image by the Novel LeNet-5 CNN Architecture." *ICCIT 2020 - 23rd International Conference on Computer and Information Technology, Proceedings*: 19–21.

Jaiswal, Aayush et al. 2021. "Classification of the COVID-19 Infected Patients Using DenseNet201 Based Deep Transfer Learning." *Journal of Biomolecular Structure and Dynamics* 39(15): 5682–89. https://doi.org/10.1080/07391102.2020.1788642.

Kathamuthu, Nirmala Devi et al. 2023. "A Deep Transfer Learning-Based Convolution Neural Network Model for COVID-19 Detection Using Computed Tomography Scan Images for Medical Applications." *Advances in Engineering Software* 175(October 2022): 103317. https://doi.org/10.1016/j.advengsoft.2022.103317.

Mohammed, Mazin Abed et al. 2020. "Benchmarking Methodology for Selection of Optimal COVID-19 Diagnostic Model Based on Entropy and TOPSIS

Methods." *IEEE Access* 8: 99115–31.

Mondal, Arnab Kumar, Arnab Bhattacharjee, Parag Singla, and A. P. Prathosh. 2022. "XViTCOS: Explainable Vision Transformer Based COVID-19 Screening Using Radiography." *IEEE Journal of Translational Engineering in Health and Medicine* 10(November 2021): 1–10.

Munusamy, Hemalatha et al. 2021. "FractalCovNet Architecture for COVID-19 Chest X-Ray Image Classification and CT-Scan Image Segmentation." *Biocybernetics and Biomedical Engineering* 41(3): 1025–38. https://doi.org/10.1016/j.bbe.2021.06.011.

Panwar, Harsh et al. 2020. "A Deep Learning and Grad-CAM Based Color Visualization Approach for Fast Detection of COVID-19 Cases Using Chest X-Ray and CT-Scan Images." *Chaos, Solitons and Fractals* 140: 110190. https://doi.org/10.1016/j.chaos.2020.110190.

Pham, Tuan D. 2020. "A Comprehensive Study on Classification of COVID-19 on Computed Tomography with Pretrained Convolutional Neural Networks." *Scientific Reports* 10(1): 1–8. https://doi.org/10.1038/s41598-020-74164-z.

Rahman, Tawsifur, Amith Khandakar, and Senior Member. 2021. "Development and Validation of an Early Scoring System for Prediction of Disease Severity in COVID-19 Using Complete Blood Count Parameters." *IEEE Access* 9: 120422–41.

Ramzy, Mohamed, Ibrahim Sherin, and M Youssef Karma. 2021. "Abnormality Detection and Intelligent Severity Assessment of Human Chest Computed Tomography Scans Using Deep Learning : A Case Study on SARS - COV - 2 Assessment." *Journal of Ambient Intelligence and Humanized Computing* (0123456789). https://doi.org/10.1007/s12652-021-03282-x.

Sakib, Sadman et al. 2020. "DL-CRC: Deep Learning-Based Chest Radiograph Classification for Covid-19 Detection: A Novel Approach." *IEEE Access* 8(July): 171575–89.

Sarker, Laboni et al. 2020. "COVID-DenseNet: A Deep Learning Architecture to Detect COVID-19 from Chest Radiology Images." *Preprints* (May). https://github.com/mmiemon/COVID-DenseNet%0Ahttp://proxy.library.stonybrook.edu/login?url=https://search.proquest.com/docview/2414040424?accountid=14172%0Ahttps://www.preprints.org/manuscript/202005.0151/v1/download%0Ahttp://linksource.ebsco.com/linking.a.

Seum, Ashek, Amir Hossain Raj, Shadman Sakib, and Tonmoy Hossain. 2020. "A Comparative Study of CNN Transfer Learning Classification Algorithms with Segmentation for COVID-19 Detection from CT Scan Images." *Proceedings of 2020 11th International Conference on Electrical and Computer Engineering, ICECE 2020*: 234–37.

Shah, Vruddhi et al. 2021. "Diagnosis of COVID-19 Using CT Scan Images and Deep Learning Techniques." *Emergency Radiology* 28(3): 497–505.

Shi, Feng et al. 2021. "Review of Artificial Intelligence Techniques in Imaging Data Acquisition, Segmentation, and Diagnosis for COVID-19." *IEEE Reviews in Biomedical Engineering* 14: 4–15.

Shukla, Prashant Kumar et al. 2020. "Efficient Prediction of Drug–Drug Interaction Using Deep Learning Models." *IET Systems Biology* 14(4): 211–16.

Silva, Pedro et al. 2020. "COVID-19 Detection in CT Images with Deep Learning: A Voting-Based Scheme and Cross-Datasets Analysis." *Informatics in Medicine Unlocked* 20: 100427. https://doi.org/10.1016/j.imu.2020.100427.

Soares, Eduardo, and Plamen Angelov. 2020. "A Large Dataset of Real Patients CT Scans for COVID-19 Identification." *Harv. Dataverse* 1: 1–8.

Tabik, S. et al. 2020. "COVIDGR Dataset and COVID-SDNet Methodology for Predicting COVID-19 Based on Chest X-Ray Images." *IEEE Journal of Biomedical and Health Informatics* 24(12): 3595–3605.

Tai, Yonghang et al. 2021. "Intelligent Intraoperative Haptic-AR Navigation for COVID-19 Lung Biopsy Using Deep Hybrid Model." *IEEE Transactions on Industrial Informatics* 17(9): 6519–27.

Tang, Shengnan, Shouqi Yuan, and Yong Zhu. 2020. "Data Preprocessing Techniques in Convolutional Neural Network Based on Fault Diagnosis towards Rotating Machinery." *IEEE Access* 8: 149487–96.

Wang, Zhao, Quande Liu, and Qi Dou. 2020. "Contrastive Cross-Site Learning with Redesigned Net for COVID-19 CT Classification." *IEEE Journal of Biomedical and Health Informatics* 24(10): 2806–13.

Wu, Yu Huan et al. 2021. "JCS: An Explainable COVID-19 Diagnosis System by Joint Classification and Segmentation." *IEEE Transactions on Image Processing* 30: 3113–26.

Yan, Qingsen et al. 2021. "COVID-19 Chest CT Image Segmentation Network by Multi-Scale Fusion and Enhancement Operations." *IEEE Transactions on Big Data* 7(1): 13–24.

Yu, Yongbin et al. 2020. "RMAF: Relu-Memristor-Like Activation Function for Deep Learning." *IEEE Access* 8: 72727–41.